THE AMERICAN SOCIETY OF MECHANICAL ENGINEERS
345 E. 47th St., New York, N.Y. 10017

97-GT-122

A NEW MODEL FOR FREE-STREAM TURBULENCE EFFECTS ON BOUNDARY LAYERS

Ralph J. Volino
Mechanical Engineering Department
U. S. Naval Academy
Annapolis, Maryland

ABSTRACT

A model has been developed to incorporate more of the physics of free-stream turbulence effects into boundary layer calculations. The transport in the boundary layer is modeled using three terms: 1) the molecular viscosity, ν; 2) the turbulent eddy viscosity, ε_T, as used in existing turbulence models; and 3) a new free-stream induced eddy viscosity, ε_f. The three terms are added to give an effective total viscosity. The free-stream induced viscosity is modeled algebraically with guidance from experimental data. It scales on the rms fluctuating velocity in the free-stream, the distance from the wall, and the boundary layer thickness. The model assumes a direct tie between boundary layer and free-stream fluctuations, and a distinctly different mechanism than the diffusion of turbulence from the free-stream to the boundary layer assumed in existing higher order turbulence models. The new model can be used in combination with any existing turbulence model. It is tested here in conjunction with a simple mixing length model and a parabolic boundary layer solver. Comparisons to experimental data are presented for flows with free-stream turbulence intensities ranging from 1 to 8% and for both zero and non-zero streamwise pressure gradient cases. Comparisons are good. Enhanced heat transfer in higher turbulence cases is correctly predicted. The effect of the free-stream turbulence on mean velocity and temperature profiles is also well predicted. In turbulent flow, the log region in the inner part of the boundary layer is preserved, while the wake is suppressed. The new model provides a simple and effective improvement for boundary layer prediction.

NOMENCLATURE

A	dimensionless coefficient in ε_f model
A^+	coefficient in Van Driest damping model
b	dimensionless coefficient in ε_f model
C_f	skin friction coefficient
c	dimensionless coefficient in ε_f model
FSTI	free-stream turbulence intensity, $[(u'^2+v'^2+w'^2)/3U_\infty^2]^{0.5}$
G	transition model parameter
H	shape factor, δ^*/θ
K	acceleration parameter, $(\nu/U_\infty^2)(dU_\infty/dx)$
k	turbulent kinetic energy
ℓ_f	mixing length for v' fluctuations
Pr_t	turbulent Prandtl number
q_o	wall heat flux
Re_x	Reynolds number based on distance from leading edge
Re_θ	momentum thickness Reynolds number
$Re_{\theta t}$	momentum thickness Reynolds number at transition start
St	Stanton number
T	temperature
U	mean streamwise velocity
u^+	U/u_τ, local velocity in wall coordinates
u'	fluctuating component of streamwise velocity
u_τ	friction velocity
v'	fluctuating component of velocity normal to wall
w'	fluctuating component of spanwise velocity
x	streamwise coordinate
y	coordinate normal to the wall
y^+	yu_τ/ν, distance from wall in wall coordinates
α	thermal diffusivity
δ	boundary layer thickness
δ^*	displacement thickness
ε	turbulence dissipation rate
ε_f	free-stream induced viscosity
ε_H	total thermal diffusivity
ε_M	total viscosity
ε_T	turbulent viscosity
ν	kinematic viscosity
θ	momentum thickness

Subscripts

∞	free-stream
f	free-stream induced

Presented at the International Gas Turbine & Aeroengine Congress & Exhibition
Orlando, Florida — June 2–June 5, 1997
This paper has been accepted for publication in the Transactions of the ASME
Discussion of it will be accepted at ASME Headquarters until September 30, 1997

INTRODUCTION

Free-stream turbulence can have a strong effect on the behavior of a boundary layer. Elevated free-stream turbulence tends to cause early transition from laminar to turbulent flow and can lead to higher skin friction and heat transfer coefficients. Highly disturbed flows are found in many applications including gas turbine engines, where free-stream turbulence intensities (FSTI) as high as 20% are possible. Given the strong effects that free-stream turbulence can have, accurate turbulence and transition models which incorporate these effects are needed for improved prediction and design. Existing turbulence models handle the FSTI in a number of ways. The simplest models do not account for the free-stream turbulence explicitly. They cannot, therefore, predict elevated heat transfer or skin friction in high FSTI boundary layers. Included are integral methods and zero-equation partial differential equation solvers which use a mixing length model for closure of the momentum equation. Higher order turbulence models, such as two-equation k-ε models, provide a means for including the free-stream turbulence effect. Equations are derived for the turbulent kinetic energy and dissipation rate, and the free-stream turbulence conditions are supplied as boundary conditions for these equations. Although these equations are derived exactly, several terms must be modeled empirically for implementation. Turbulence is modeled as entering the boundary layer from the free-stream through a diffusion process. This turbulence then raises the level of transport in the boundary layer, resulting in higher skin friction and heat transfer coefficients. It also leads to boundary layer transition.

Two-equation models must produce the correct qualitative end results. Turbulence is put into the boundary layer, and this will tend to cause transition and higher skin friction and heat transfer. The mechanism by which the turbulence enters the boundary layer in existing models may not be correct, however. If the mechanism is not correct, the constants in the models may still be tuned to give good predictions in some flows, but there is no reason to expect the models to be robust over all conditions. It is also questionable whether continued work with such models will lead to improvement, particularly in the area of transition. Increasing the FSTI in a k-ε simulation will correctly move transition upstream, but current models are still often poor predictors of transition (Mayle, 1991). This is evidenced by the comparisons in Savill (1992). Existing models generally predict transition start too far upstream and too short a transition zone.

Recent work suggests that diffusion may not be the primary mechanism by which free-stream turbulence influences the boundary layer. Volino and Simon (1994) considered transitional boundary layers under both low (0.6%) and high (8%) FSTI conditions. They documented spectra of the fluctuating streamwise velocity, u′, the fluctuating normal component of velocity, v′, and the turbulent shear stress, -u′v′, at several positions in the boundary layer and in the free-stream. In the pre- and early-transitional boundary layers they found that the peak energy in the boundary layer u′ spectra occurred at the same frequency as the peak in the free-stream v′ spectra. This was observed under both high and low FSTI conditions. The boundary layer u′ fluctuations were believed to be caused by the "splat mechanism" proposed by Bradshaw (1994). In the splat mechanism, free-stream eddies buffet the boundary layer. A negative v′ fluctuation in the free-stream compresses the boundary layer momentarily, forcing high speed fluid from the outer region closer to the wall. This results in a positive u′ fluctuation in the boundary layer. The free-stream acts directly on the boundary layer. The mechanism does not involve turbulence diffusion. The splat mechanism consists mainly of "inactive motions," i.e. motions that do not lead to turbulent transport. Once the free-stream eddy passes, the boundary layer rebounds to its original state, with little net effect. This compression and release of the boundary layer may, however, lead to some turbulent mixing. Under high FSTI conditions, Volino and Simon (1994, 1995a) found significant levels of -u′v′ in the upstream, pre-transitional boundary layer, and it occurred at the frequencies of the peak v′ in the free-stream unsteadiness. This upstream -u′v′ was of lower energy and lower frequency than the -u′v′ in the fully-turbulent boundary layer downstream. The upstream -u′v′ still had an impact on the upstream boundary layer, however, influencing the mean velocity and temperature profiles and enhancing the skin friction and heat transfer (Volino and Simon, 1995b).

Moss and Oldfield (1996) provide more direct evidence of the effect of the free-stream on the boundary layer. They considered FSTI up to 12%, recording simultaneous traces of instantaneous free-stream velocity and instantaneous wall heat flux. The correlation coefficient between the unsteady velocity and heat flux was as high as 50%. The spectra of the two signals were similar at low wavenumbers, but at higher wavenumbers the heat flux appeared unaffected by the free-stream. Instantaneous Nusselt numbers fluctuated between a low level similar to that seen in low-FSTI turbulent boundary layers and a high level which was up to 100% higher. The transition between the two levels occurred at a low frequency, which was associated with the free-stream turbulence. Smaller, higher frequency fluctuations within the heat flux signal were associated with turbulence within the boundary layer. Velocity spectra taken in the free-stream and near the wall were nearly identical, suggesting that free-stream eddies were "penetrating right through the velocity-defect part of the boundary layer." The turbulent eddy structure of the boundary layer was believed to be dominated by high free-stream turbulence, and this was believed to be the main heat transfer enhancing mechanism.

Thole and Bogard (1996) considered boundary layers with FSTI ranging from 10 to 20%. At low wavenumbers they found that the free-stream u′ spectra and the boundary layer spectra down to $y^+=15$ were nearly identical. At higher wavenumbers the FSTI level had little effect on the near wall spectra. At 12% FSTI the near wall spectra exhibited a double peak, with the lower frequency peak matching the peak frequency in the free-stream spectra. The higher frequency peak was associated with boundary layer generated turbulence.

Mayle and Schultz (1996) developed a "laminar kinetic energy" equation for pre-transitional flows, and showed that pressure fluctuations, not diffusion, are the primary mechanism for turbulence entering the boundary layer.

The studies described above all suggest a direct link between free-stream and boundary layer fluctuations. They also show a distinct frequency separation between fluctuations induced by the free-stream and fluctuations generated within the boundary layer by near wall production. Although the u′v′ correlation is lower in the free-stream induced fluctuations than in the boundary layer generated turbulence, the free-stream has a significant and direct role in enhancing heat transfer. The diffusion mechanism used in current

turbulence models does not appear to be supported by the experimental results.

In the present study a new method is proposed to model the direct link between the free-stream and boundary layer. A model is developed, as motivated by the experimental data, and then tested against several experimental data sets.

TURBULENCE MODEL

The two distinct scales observed in the experimental data suggest a separate treatment of the boundary-layer-generated and free-stream-induced turbulence. For modeling purposes, the two scales are assumed independent of each other except for their mutual influence and dependence on the mean streamwise velocity profile. The effect of the near-wall-generated turbulence is captured with an existing turbulence model. A new model is developed below for the free-stream effect.

The "splat mechanism" proposed by Bradshaw (1994) and discussed by Volino and Simon (1994) suggests that the level of free-stream induced u′ fluctuations in a boundary layer should depend on the level of v′ fluctuations, a characteristic length, ℓ_v, associated with these fluctuations, and the mean velocity gradient, dU/dy. A v′ fluctuation transports a packet of fluid some distance ℓ_v across the mean streamwise velocity gradient, resulting in a fluctuation $u' \propto \ell_v dU/dy$. The spectral results of Volino and Simon (1994) suggest that the turbulent transport induced by these fluctuations varies with the magnitude of the u′ fluctuations.

The magnitude of the free-stream induced v′ fluctuations in the boundary layer can be inferred from an experimental v′ profile in a high FSTI flow. Figure 1 shows a typical example from Volino and Simon (1995a). The value of v′ drops from a maximum near the wall to a minimum at $y/\delta=0.25$, before rising to the free-stream value. The near wall peak can be associated with near wall turbulence production. The decrease from the free-stream to $y/\delta=0.25$ suggests that the free-stream effect diminishes as the boundary layer is penetrated and the wall is approached. This effect should approach zero at the wall. The free-stream induced v′ is assumed to scale with the distance from the wall, y, and inversely with the boundary layer thickness, δ.

If the length scale ℓ_v is assumed to scale with v′, y and δ, the above argument suggests the following form for the free-stream induced shear stress, $-u'v'_f$.

$$-u'v'_f = Av'_\infty \frac{y^b}{\delta^c}\frac{dU}{dy} \qquad (1)$$

where A, b and c are dimensionless constants. To be dimensionally correct, c=b-1 The form of Eqn. (1) suggest a free-stream induced eddy viscosity of the form:

$$\varepsilon_f = Av'_\infty \frac{y^b}{\delta^{b-1}} = Av'_\infty \delta\left(\frac{y}{\delta}\right)^b \qquad (2)$$

The value of v'_∞ may be allowed to vary in the streamwise direction to model the decay of the free-stream turbulence. In the present study, however, most of the experimental comparison cases showed only a small variation in v'_∞ with position, so v'_∞ was assumed constant at an upstream value for all calculations. The constants A and b are determined empirically. For two-dimensional boundary layers on flat walls with grid generated turbulence and FSTI<8%, A=0.41 and b=2.5 were determined based on a best overall fit to the laminar and turbulent Stanton number data of Blair (1982, 1983). In laminar boundary layers ε_f is assumed to act in combination with the molecular viscosity, ν. In turbulent boundary layers it is assumed to act in combination with the molecular viscosity and turbulent viscosity, ε_T. This is discussed further below.

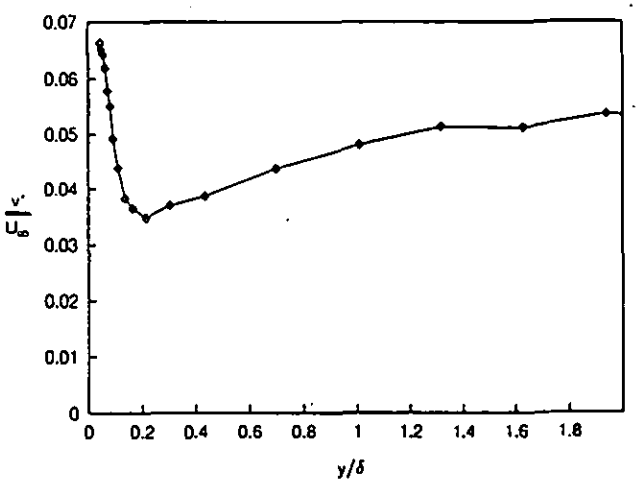

Fig. 1: Typical v' Profile from a High FSTI Boundary Layer

The above development, although guided by experimental observations, is recognized as speculative. Its utility is demonstrated by the model's ability to improve the match of calculations to experimental data.

IMPLEMENTATION OF THE MODEL

The free-stream eddy viscosity proposed in Eqn. (2) is independent of the near-wall turbulence model (e.g. k-ε or mixing length) and the computational method used in a simulation. In this study the new free-stream model (henceforth referred to as the FS model) is implemented along with a mixing length turbulence model. Since a mixing length model alone has no way of incorporating free-stream effects, use of one provides a clear and relatively simple test of the FS model. Computations are done using the TEXSTAN code referenced in Kays and Crawford (1993). TEXSTAN is an updated version of the STAN5 code presented by Crawford and Kays (1976). It is a two-dimensional, parabolic boundary layer code based on the Patankar and Spalding (1970) method. The mixing length model included in the TEXSTAN code, which includes the Van Driest (1956) near wall damping model with a variable A^+ parameter, is utilized. Details are available in Kays and Crawford (1993).

The total viscosity, ε_M, used in the solution of the momentum equation is the sum of the molecular, turbulent and free-stream contributions:

$$\varepsilon_M = \nu + \varepsilon_T + \varepsilon_f \qquad (3)$$

where ε_T is provided by the mixing length model. In laminar flows this reduces to

$$\varepsilon_M = \nu + \varepsilon_f \qquad (4)$$

The energy equation is solved using the total thermal diffusivity, ε_H, where

$$\varepsilon_H=\alpha+(\varepsilon_T+\varepsilon_f)/Pr_t \quad (5)$$

and Pr_t is the turbulent Prandtl number. A variable Pr_t model recommended by Kays and Crawford (1993) is used. Heat transfer calculations depend strongly on the choice of Pr_t. The Kays and Crawford model produces good agreement with near wall ($y^+<100$) mean temperature profile data, in wall coordinates, at all of the FSTI considered in this study, independent of whether the FS model is in use. Changing the Pr_t model produced changes in the slope and magnitude of the mean temperature profiles in the inner part of the boundary layer, which were not supported by the experimental data. The Kays and Crawford (1993) model is, therefore, used in all computations in this study.

Transition model

Although development of a transition model is not the purpose of this paper, a transition model was needed for evaluation of the FS model in transitional and early turbulent boundary layers. The most reliable models currently available depend on empirical correlations for transition start and end. Transition was initiated in the present calculations by turning on ε_T when the momentum thickness Reynolds number, Re_θ, exceeded the value given by a correlation. Park and Simon (1987) recommended use of the Abu-Ghannam and Shaw (1980) correlation,

$$Re_{\theta t}=163+\exp(6.91-FSTI) \quad (6)$$

for transition start with mixing length models. Schmidt and Patankar (1991) also used this correlation in the development of their "Production Term Modification" (PTM) k-ε transition model, which provides improved transition prediction over standard k-ε calculations. Mayle (1991) stated that the lower limit of 163 on $Re_{\theta t}$ in Eqn. (6) is artificial and proposed the equation

$$Re_{\theta t}=400(FSTI)^{-5/8} \quad (7)$$

This is similar to the correlation

$$Re_{\theta t}=460(FSTI)^{-0.65} \quad (8)$$

given by Hourmouziadis (1989). Recognizing that the correlations were developed for different ranges of FSTI, Eqns. (6) and (8) were used for cases with FSTI less than and greater than 4.5% respectively. Additionally, transition was not allowed to begin if the acceleration parameter K was above 3×10^{-6}, as suggested by Mayle (1991). This last restriction has no effect at low FSTI, since the strong acceleration suppresses the growth of the boundary layer, keeping Re_θ below $Re_{\theta t}$. At high FSTI, however, where $Re_{\theta t}$ is itself low, the restriction can move transition start downstream.

TEXSTAN provides for a gradual transition with the mixing length model by modifying the Van Driest (1956) damping term. This is accomplished by setting the A^+ term to 300 at the start of transition, then allowing it to gradually decrease to its equilibrium value ($A^+=25$ for unaccelerated flow) at the end of transition. This was found to still produce too abrupt a transition, so a further modification was implemented. In the range $Re_{\theta t} < Re_\theta < 2.667Re_{\theta t}$ (with the 2.667 factor coming from the Abu-Ghannam and Shaw, 1980 model for transition length), Eqns. (3) and (5) were modified to

$$\varepsilon_M=\nu+G\varepsilon_T+\varepsilon_f \quad (9)$$

$$\varepsilon_H=\alpha+(G\varepsilon_T+\varepsilon_f)/Pr_t \quad (10)$$

with

$$G=(Re_\theta-Re_{\theta t})/(1.667*Re_{\theta t}) \quad (11)$$

This might be thought of as a crude intermittency model. Although G does not match the shape of typical intermittency distributions (e.g. Abu Ghannam and Shaw, 1980), it does vary smoothly with Re_θ, increasing from zero to one, as does the intermittency.

Initial Conditions

All computations were started at x=0.0001 m ($Re_x\approx100$) with a Blasius velocity profile and a uniform temperature profile. The boundary layer thickness was set to 4×10^{-5} m using a nonuniform grid with forty points. Testing with different starting profiles and finer grids showed that results were independent of the initial conditions and grid to within 0.5%.

RESULTS

The behavior of the model is demonstrated with a series of runs simulating air flow with a constant U_∞=20 m/s and T_∞=300K along a 2 m long plate. The wall boundary condition was a constant heat flux of 200 W/m^2. Simulations were run with 0, 1, 5 and 10% FSTI. Skin friction coefficient and Stanton number results are presented in Fig. 2 for simulations with the boundary layer assumed turbulent from the leading edge. At zero FSTI the model reduces to the standard mixing length model, and the results agree with correlations presented in Kays and Crawford (1993). At 1% FSTI, both C_f and St are about 5% above the zero FSTI conditions. At 10% FSTI, C_f and St are 15% above the zero turbulence results. Also shown in Fig. 2 are Stanton numbers for the same cases, but with laminar flow (ε_T set to zero). At $Re_x=2.5\times10^6$, 25% and 45% enhancements in St are seen for the 1% and 10% FSTI cases respectively. Although laminar flow under these conditions would not be observed in practice, similar results would be expected in strongly accelerated, high FSTI flows, where extended laminar and transition regions would be present even under high FSTI conditions. Examples of such cases from Blair (1982) and Volino and Simon (1995b) are presented below.

The effect of the free-stream turbulence on the mean streamwise velocity profiles is shown in Fig. 3 for fully-laminar and fully-turbulent simulations. Profiles are presented in wall coordinates at $Re_x=0.5\times10^6$ (Re_θ between 400 and 600) for the laminar runs and at $Re_x=2.5\times10^6$ (Re_θ between 4700 and 5400) for the turbulent simulations. The free-stream turbulence causes the laminar profiles to deviate from the zero FSTI, Blasius profile, and suppresses the wake in the turbulent profiles, in agreement with experimental data (e.g. Blair, 1983). Similar results are observed in the mean temperature profiles. The log region of the turbulent profiles is unaffected by the free-stream, in agreement with experimental results such as those of Thole and Bogard (1996). This lends support to the form of ε_f given by Eqn. (2).

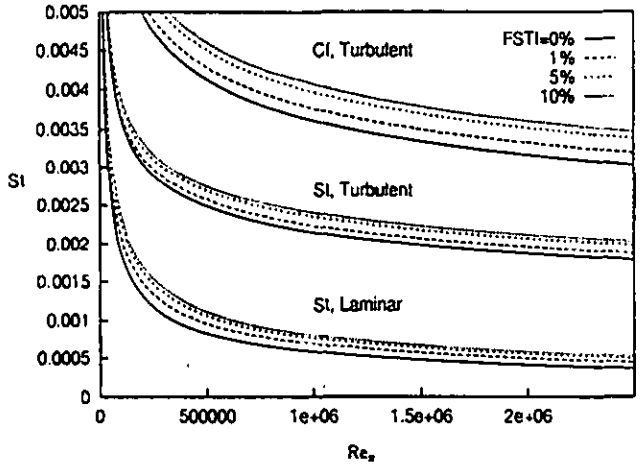

Fig. 2: FS Model Stanton No. and Skin Friction Coefficient Predictions for Unaccelerated Flow on a Flat Plate

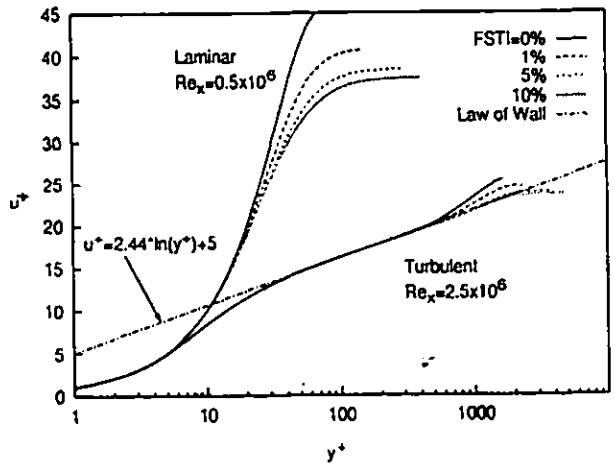

Fig. 3: FS Model Velocity Profile Predictions for Unaccelerated Flow on a Flat Plate

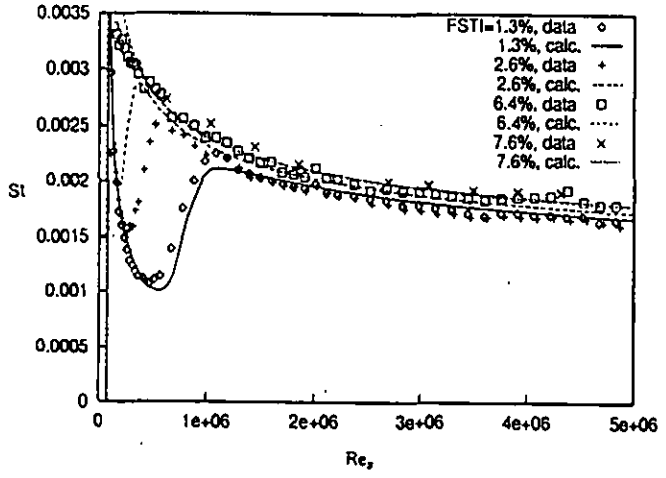

(a) FS Model

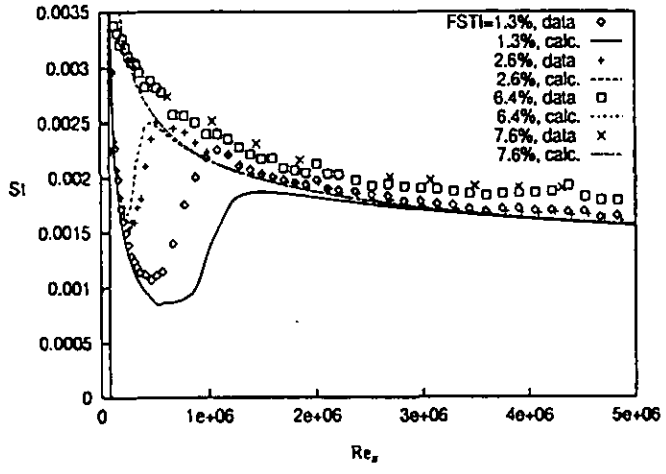

(b) Standard Mixing Length Model

Fig. 4: Comparison of Stanton No. Predictions to Unaccelerated Flow Data of Blair (1983)

Comparison to Experimental Data

The above results exhibit the correct trends, but a comparison to experimental data is needed to quantitatively validate the model. Data from flat and concave-curved wall cases, and from accelerated and unaccelerated flows were chosen. Free-stream turbulence levels up to 8% were considered. All experimental results are for flows of room temperature air along walls with constant flux heating downstream of a short unheated starting length. Attention is focused on Stanton number data and mean velocity and temperature profiles.

Unaccelerated flow over flat walls. Blair (1983) considered unaccelerated flow along a flat wall with U_∞=30 m/s and q_o=880 W/m^2 downstream of a 4.3 cm long unheated starting length. Data are tabulated in Blair (1981a). Free-stream turbulence intensities of 1.3, 2.6, 6.4 and 7.6% were generated with grids. Experimental Stanton number data are compared to calculated results in Fig. 4a. The same data are compared to standard mixing length calculations (ε_f set to zero) in Fig. 4b. The free-stream turbulence has only a small effect in the laminar region in these flows, and the laminar data are well predicted in both sets of calculations. In the turbulent region, the FS model provides an improved match to the data. For the 1.3% FSTI case, the standard model predicts St about 5% too low, while the FS model is about 2% too high. The standard model provides a better prediction of the 2.6% FSTI case, but the experimental data show the wrong trend with FSTI for this case, with St below the level of the 1.3% case. At the 6.4% and 7.6 % FSTI levels, the standard model predicts Stanton number between 10 and 14% too low, while the FS model predicts St within 2% of the data. Schmidt and Patankar (1991) provide comparisons to these data sets with their k-ε, PTM model. Their results are nearly identical to those of Fig. 4a, both in the prediction of transition (expected since both are based on the Abu-Ghannam and Shaw, 1980 model) and in the prediction of heat transfer enhancement due to the FSTI effect.

Figure 5 shows comparisons of mean velocity and temperature profile data to the FS and standard mixing length calculations for a

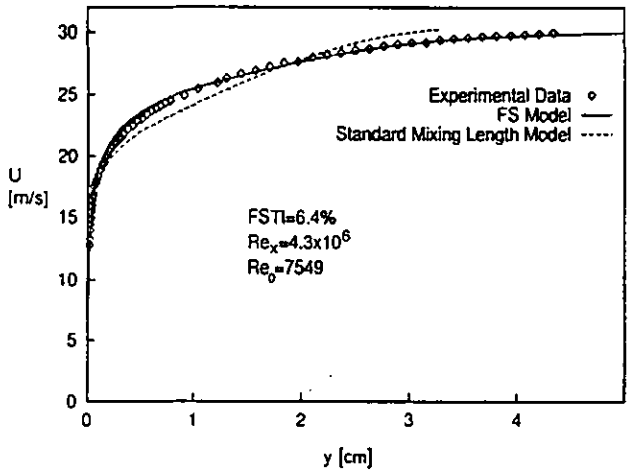

(a) Velocity Profile

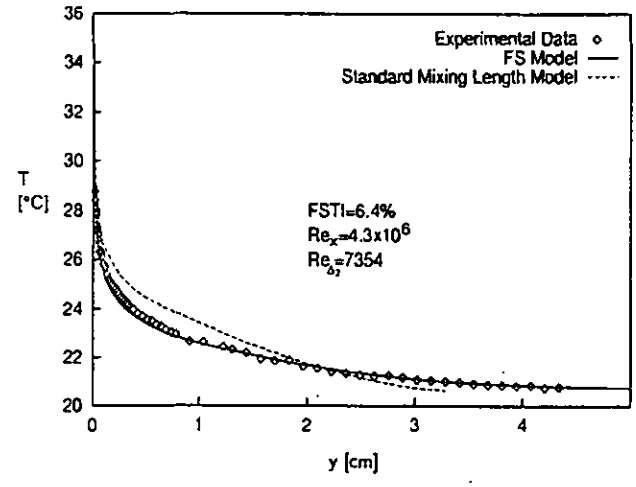

(b) Temperature Profile

Fig. 5: Comparison of Calculated Profiles to Unaccelerated Flow Data of Blair (1983)

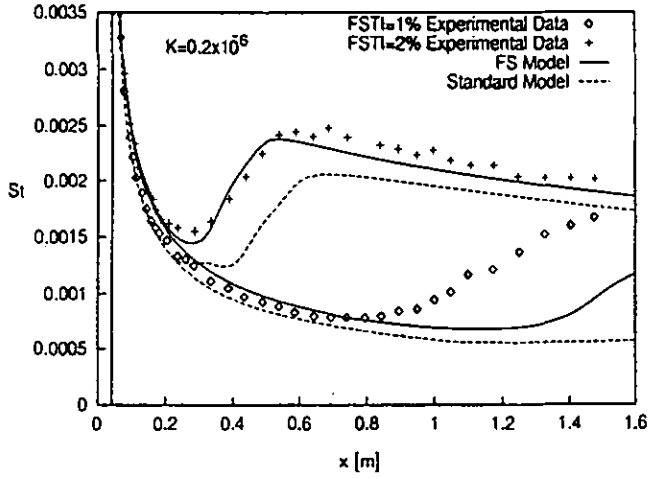

(a) K=0.2×10^{-6}

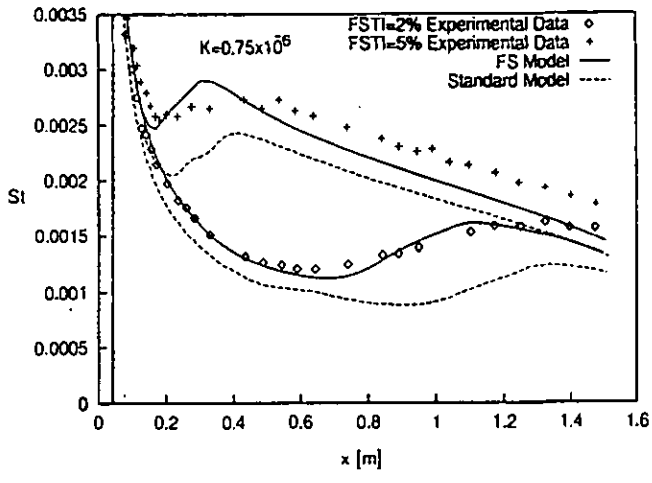

(b) K=0.75×10^{-6}

Fig. 6: Comparison of FS Model and Standard Mixing Length Stanton No. Predictions to Accelerated Flow Data of Blair (1982)

typical location from the fully-turbulent zone of the 6.4% FSTI case. The FS model provides a clear improvement. The elevated FSTI leads to faster growth of the boundary layer, which is well captured. The wall temperature is predicted to within 1% of the wall-to-free-stream difference by the FS model, while the standard model prediction was 13% high. The shape factor, H, from the measured velocity profile was 1.33, while the value predicted by the FS and standard models were 1.29 and 1.42 respectively.

Accelerated flow over flat walls. Blair (1982) considered flow over a flat wall subject to favorable pressure gradients. Data are tabulated in Blair (1981b). At a constant acceleration parameter $K=0.2\times10^{-6}$ and inlet U_∞=15.9 m/s, cases with 1 and 2% FSTI were considered. At a constant $K=0.75\times10^{-6}$ and inlet U_∞=10.1 m/s, cases with 2 and 5% FSTI were documented. In all four cases the wall heat flux was approximately 500 W/m^2. Stanton numbers calculations using the FS and standard mixing length models are compared to the data in Fig. 6. At $K=0.2\times10^{-6}$ and 1% FSTI (Fig. 6a), the models are comparable in the laminar region, predicting the data to within about 8%. Both models predict too late a transition. At $K=0.2\times10^{-6}$ and 2% FSTI, the FS model is clearly better. It matches the laminar data, predicts the transition well, and is about 4% low in the turbulent region. The standard mixing length model is 12% low in the laminar and turbulent regions and predicts a late transition. At $K=0.75\times10^{-6}$ and 2% FSTI (Fig. 6b) the FS model matches the data to within about 3% in the laminar and transition regions while the standard model is about 15% low in the laminar region and predicts a late transition. At 5% FSTI the FS model is about 9% low in the turbulent region, while the standard model is about 18% low.

Schmidt and Patankar (1988, 1991) also simulated these accelerated cases with their PTM model. At the lower K, they predict the 1% FSTI case well, including the transition. In the 2% FSTI case, their result is nearly identical to the prediction of the FS

model in Fig. 6a. At $K=0.75\times10^{-6}$ with 2% FSTI, the PTM model predicts Stanton numbers 20% low in the laminar region and transition about 0.3 m too far upstream. Schmidt and Patankar (1991) noted low St predictions in the laminar region of other strongly accelerated flows. At 5% FSTI the PTM model produces results very similar to those of the FS model in Fig. 6b.

In summation, for the flat wall cases considered here, the new model is a clear improvement over the standard mixing length model. It correctly predicts the effects of free-stream turbulence. The model behaves very similarly to the more complex PTM k-ε model and in some cases produces a better result.

Modeling of curvature effects

To demonstrate an extension of the FS model, the effects of streamwise curvature are considered. Streamwise concave curvature is inherently destabilizing and can lead to higher heat transfer rates. Kestoras and Simon (1995) stated that when concave curvature and high FSTI are combined, the free-stream eddies are able to penetrate closer to the wall than in a flat wall flow, resulting in significantly higher turbulent transport within the boundary layer. They studied an 8% FSTI flow moving from a concave wall onto a flat recovery wall, and measured an almost immediate drop in turbulence within the boundary layer as the flow moved onto the flat wall. This rapid recovery further suggests that the effect of the free-stream on the boundary layer is a direct one and not due to turbulent diffusion.

If the enhanced transport in concave-wall boundary layers is in part due to a closer penetration of free-stream eddies toward the wall, an adjustment of the profile of ε_f might capture the effect. To maintain the level of ε_f at the edge of the boundary layer while increasing the effect within the boundary layer, the constant b in Eqn. (2) can be lowered while the constant A is held fixed. Kim et al. (1992) investigated boundary layers with 8% FSTI along both a flat wall and a concave wall with a constant radius of curvature of 1 m. In the turbulent region of the flow, an FS model simulation of the flat wall case produced Stanton numbers in agreement with the experimental data to within 5%. For the concave wall case, it was found that changing the constant b to 1.5 produced a good match to the turbulent flow data. The 8% FSTI alone (with b set to the 2.5 flat wall value) produced an 11% rise in Stanton number above a zero FSTI calculation, and the curvature effect (b set to 1.5 with FSTI=8%) produced an additional 16% increase, for a total rise of 27% over a zero FSTI flat wall flow.

To test the concave wall model, accelerated flow data acquired by Volino and Simon (1995b, 1995c) along the same 1 m radius of curvature wall used in the Kim et al. (1992) study were considered. The following three cases were simulated, all with a nominal 8% FSTI at the inlet to the test section.

Case	Inlet U_∞	Acceleration	Wall Heat Flux
1	7.5 m/s	$K=0.75\times10^{-6}$ constant	76 W/m^2
2	9.6 m/s	$dU_\infty/dx=28$ s^{-1} constant	380 W/m^2
3	4.9 m/s	$dU_\infty/dx=13.6$ s^{-1} constant	180 W/m^2

The mixing length turbulence model, as described above, was used for the calculations with no additional curvature correction. Stanton numbers for the three cases are presented in Fig. 7. The transition is not well predicted in Case 1, but the calculated results are within 4% of the data at the downstream stations. The calculated results are

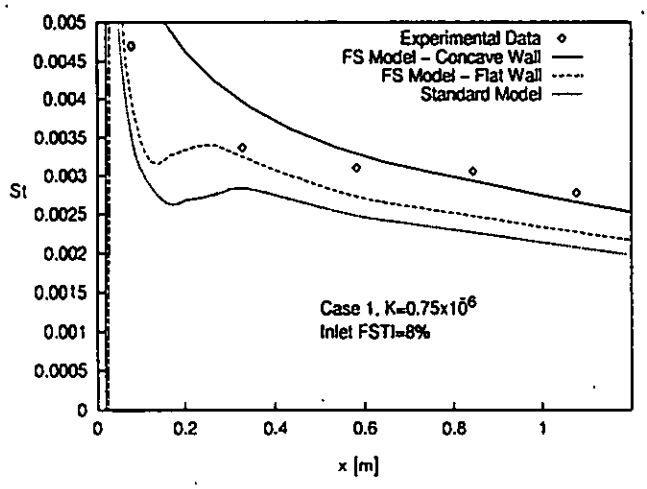

(a) Case 1

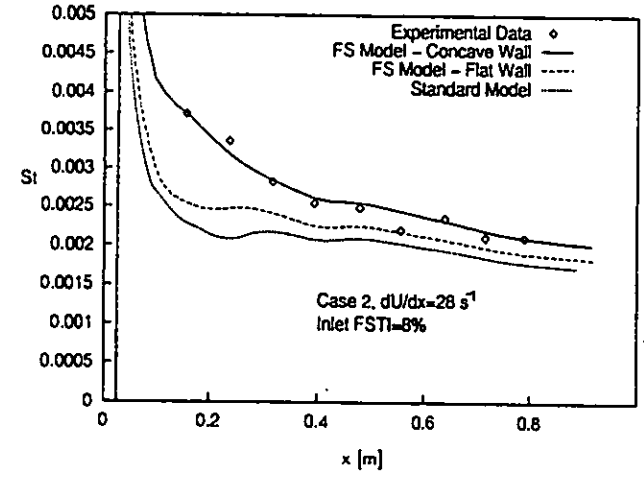

(b) Case 2

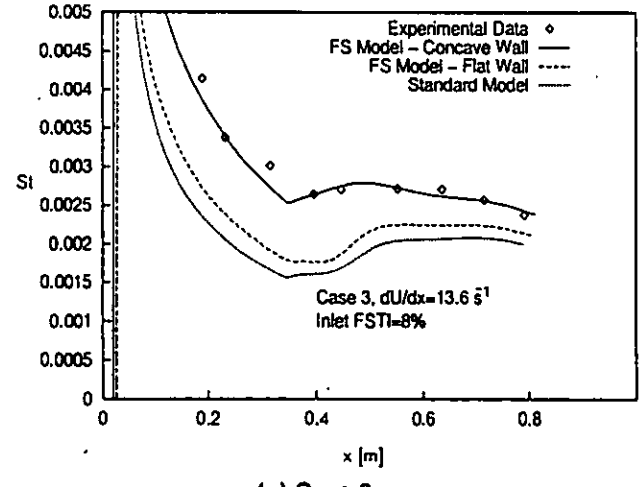

(c) Case 3

Fig. 7: Comparison of FS Model and Standard Mixing Length Stanton No. Predictions to Accelerated, Concave Wall Data of Volino and Simon (1995c)

17% higher than those from a flat wall simulation with the FS model, and 28% higher than those predicted with the standard mixing length model. The calculations for Cases 2 and 3 are in good agreement with the data in all regions of the flow. Stanton numbers are well above the values predicted by a flat-wall FS calculation or the standard mixing length model. Volino and Simon (1995c) stated that the curvature effect in these cases was probably small, since the acceleration kept the boundary layer thin. The present computations suggest that the curvature effect may have actually been large. An experiment on a flat wall under the FSTI and acceleration conditions of Case 3 would be an interesting check of this result. Cases 2 and 3 include extended non-turbulent regions due to the strong acceleration, which delays the start of transition in spite of the high FSTI. In this "disturbed laminar" region, the FS model correctly predicts a rise in Stanton numbers by as much as 65% above a laminar calculation. Figure 8 shows temperature profiles from two stations of Case 3. At the upstream station the flow is pre-transitional (ε_T=0). All deviation from laminar behavior is due to the free-stream effect. The profile shape, boundary layer thickness and wall temperature are all well predicted. At the downstream station the flow is fully turbulent. As at the upstream station the calculated profile matches the data well, and represents a substantial improvement over the standard mixing length model.

DISCUSSION

The above results suggest the usefulness of the FS model. In the cases considered, results were good and comparable to those produced with a k-ε model. The FS model holds advantages over existing k-ε models. When used in conjunction with a mixing length model, it is less computationally intense. The FS model is also simpler, and is believed to model the physics of the free-stream - boundary layer interaction better than the diffusion model assumed in k-ε computations. The location of the start of calculations is less important with the FS model than with standard models since the problem of allowing sufficient distance for diffusion of turbulence into the boundary layer is not an issue. Regardless of the comparison to k-ε models, mixing length models are still the models of choice in many Navier-Stokes calculations (Lakshminarayana, 1996) and the FS model provides a straightforward means of incorporating free-stream effects into these calculations.

While the comparisons presented above are generally good, they are limited. The purpose of the present work is to introduce the model and demonstrate its utility. Further work is still needed. All comparisons were to flows with grid generated turbulence in which the integral length scale based on v'_∞ was 1 to 3 times the boundary layer thickness. Several investigators (e.g. Hancock and Bradshaw, 1989) have concluded that both free-stream intensity and length scale are important, and that large free-stream eddies have a greater effect on the boundary layer than smaller scale eddies. One or both of the constants in Eqn. (2) might be a function of the free-stream integral length scale. Comparison to flows with different types of free-stream turbulence are needed.

The curvature correction presented above demonstrates the utility of the FS model and the way it may be modified based on an understanding of the flow. What one can say about the correction is, however, limited since the flows considered were all from the same test wall at the same nominal FSTI. One might speculate that the constant b in Eqn. (2) is a function of the radius of the curvature of

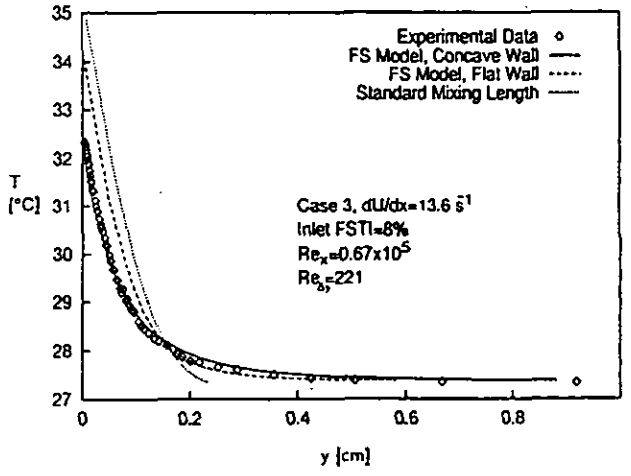

(a) Laminar Region

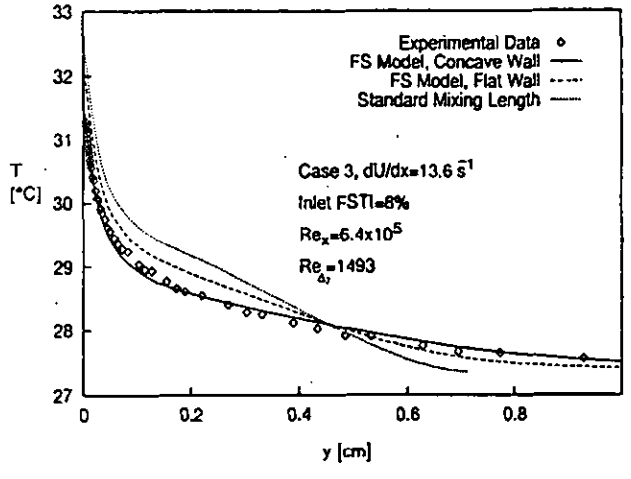

(b) Turbulent Region

Fig. 8: Comparison of FS Model and Standard Mixing Length Temperature Profile Predictions to Accelerated, Concave Wall Data of Volino and Simon (1995c)

the wall and possibly the free-stream turbulence level, but only further comparisons will confirm or deny this.

A final point is that the cases chosen for comparison were deliberately selected as relatively simple cases in which a mixing length calculation would be possible. No attempt was made, for example, to simulate an adverse pressure gradient flow, where a mixing length calculation would most likely fail, with or without the FS model correction. The FS model is in no way limited, however, to implementation with a mixing length model. If the FS model does capture the physics of the free-stream effect better than a conventional diffusion model, it may prove a useful addition to higher order turbulence models.

CONCLUSIONS

The FS model has been introduced and successfully tested in comparisons to a range of experimental data sets. The model is based

on experimental observations, which suggest a direct link between free-stream turbulence and turbulent transport in the boundary layer. This is believed to be an improvement over the diffusion mechanism assumed in existing higher order turbulence models. The FS model can be used in combination with any existing turbulence model, and provides a means for incorporating free-stream turbulence effects into mixing length calculations. Further testing and development of the model are warranted.

REFERENCES

Abu-Ghannam, B.J. and Shaw, R. (1980). "Natural Transition of Boundary Layers - The Effects of Turbulence, Pressure Gradient and Flow History," *J. Mech. Eng. Sci.*, Vol. 22, No. 5, pp. 213-228.

Blair, M.F. (1981a). "Final Data Report - Vol. I - Velocity and Temperature Profile Data for Zero Pressure Gradient, Turbulent Boundary Layers," United Technologies Research Center report R81-914388-15.

Blair, M.F. (1981b). "Final Data Report - Vol. II - Velocity and Temperature Profile Data for Accelerating, Transitional Boundary Layers," United Technologies Research Center report R81-914388-16.

Blair, M.F. (1982). "Influence of Free-Stream Turbulence on Boundary Layer Transition in Favorable Pressure Gradients," *J. Engineering for Power*, Vol. 104, pp. 743-750.

Blair, M.F. (1983). "Influence of Free-Stream Turbulence on Turbulent Boundary Layer Heat Transfer and Mean Profile Development, Part-I, Experimental Data, Part-II Analysis of Results," *J. Heat Transfer*, Vol. 105, pp. 33-47.

Bradshaw, P. (1994). "Turbulence: the chief outstanding difficulty of our subject," *Exp. in Fluids*, Vol. 16, pp. 203-216.

Crawford, M.E. and Kays, W.M. (1976). "STAN5 - A Program for Numerical Computation of Two-Dimensional Internal and External Boundary Layer Flows," NASA CR 2742.

Hancock, P. and Bradshaw, P. (1989). "Turbulence Structure of a Boundary Layer beneath a Turbulent Free-Stream," *J. Fluid Mech.*, Vol. 205, pp. 45-76.

Hourmouziadis, J. (1989). "Aerodynamic Design of Low Pressure Turbines," AGARD Lecture Series, 167.

Kays, W.M. and Crawford, M.E. (1993). *Convective Heat and Mass Transfer*, 3rd ed., McGraw-Hill Inc., New York.

Kestoras, M.D. and Simon, T.W. (1995). "Effects of Free-Stream Turbulence Intensity on a Boundary Layer Recovering from Concave Curvature Effects," *J. Turbomachinery*, Vol. 117, pp. 240-247.

Kim, J., Simon, T.W., and Russ, S.G. (1992). "Free-Stream Turbulence and Concave Curvature Effects on Heated Transitional Boundary Layers," *J. Heat Transfer*, Vol. 114, pp. 338-347.

Lakshminarayana, B. (1996). *Fluid Dynamics and Heat Transfer of Turbomachinery*, John Wiley & Sons, New York.

Mayle, R.E. (1991). "The Role of Laminar-Turbulent Transition in Gas Turbine Engines," *J. Turbomachinery*, Vol. 113, pp. 509-537.

Mayle, R.E. and Schultz, A. (1996). "The Path to Predicting Bypass Transition," ASME paper 96-GT-199.

Moss, R.W. and Oldfield, M.L.G. (1996). "Effect of Free-Stream Turbulence on Flat-Plate Heat Flux Signals: Spectra and Eddy Transport Velocities," *J. Turbomachinery*, Vol. 118, pp. 461-467.

Park, W. and Simon, T.W. (1987). "A Test of the MLH Models for Prediction of Convex-Curved Transitional Boundary Layer Heat Transfer Behavior," Proceedings of the 1987 ASME-JSME Thermal Engineering Joint Conference, Vol. 3, pp. 349-360.

Patankar, S.V. and Spalding, D.B. (1970). *Heat and Mass Transfer in Boundary Layers*, 2nd ed., Intertext, London.

Savill, A.M. (1992). "A Synthesis of T3 Test Case Predictions," *Numerical Simulation of Unsteady Flows and Transition to Turbulence*, O. Pironneau et al., ed., Cambridge University. Press, pp. 404-442.

Schmidt, R.C. and Patankar, S.V. (1988). "Two-Equation Low-Reynolds-Number Turbulence Modeling of Transitional Boundary Layer Flows Characteristic of Gas Turbine Blades," NASA CR 4145.

Schmidt, R.C. and Patankar, S.V. (1991). "Simulating Boundary Layer Transition with Low-Reynolds-Number k-ε Turbulence Models, Part 1 - An Evaluation of Prediction Characteristics, Part 2 - An Approach to Improving the Predictions," *J. Turbomachinery*, Vol. 113, pp. 10-26.

Thole, K.A. and Bogard, D.G. (1996). "High Freestream Turbulence Effects on Turbulent Boundary Layers," *J. Fluids Engineering*, Vol. 118, pp. 276-284.

Van Driest, E.R. (1956). "On Turbulent Flow Near a Wall," *J. Aero. Sci.*, Vol. 23, pp. 1007-1011.

Volino, R.J. and Simon, T.W. (1994). "Transfer Functions for Turbulence Spectra," *Unsteady Flows in Aeropropulsion*, ASME AD-Vol. 40, pp. 147-155.

Volino, R.J. and Simon, T.W. (1995a). "Measurements of Turbulent Transport in Transitional Boundary Layers Under High Free-Stream Turbulence and Strong Acceleration Conditions," Proceedings of the 10th Symposium on Turbulent Shear Flows, Vol. 2, pp. P2-43 - P2-48.

Volino, R.J. and Simon, T.W. (1995b). "Boundary Layer Transition under High Free-Stream Turbulence and Strong Acceleration Conditions: Mean Flow Results," Proceedings of the 4th ASME/JSME Thermal Engineering Joint Conference, Vol. 1, pp. 335-342.

Volino, R.J. and Simon, T.W. (1995c). "Measurements in Transitional Boundary Layers Under High Free-Stream Turbulence and Strong Acceleration Conditions," NASA CR 198413.